

Ruby Xenocrystals in Dacite from Central Mexico

Luis Enrique Ortiz Hernández^{1,2}  and José C. Escamilla-Casas^{1*} 

Abstract

The occurrence of 1-2 cm in diameter, anhedral xenocrystals of red corundum (ruby) in a dacitic lava-flow from central Mexico -in the state of Hidalgo- has been recorded. Geochemically, this dacite nearly resembles adakitic rock ($\text{SiO}_2=63.73\ 66.64\ \text{wt \%}$), with low alumina contents ($\text{Al}_2\text{O}_3=14.38\ 14.93\ \text{wt \%}$), sodium ($\text{Na}_2\text{O}=3.29\ 3.57\ \text{wt \%}$) and titanium ($\text{TiO}_2=0.55\ 0.60\ \text{wt \%}$), slightly peraluminous ($\text{A/CNK}=1.04\ 1.17$) and moderately potassic ($\text{K}_2\text{O}=1.90-2.04\ \text{wt \%}$; $\text{K}_2\text{O}/\text{Na}_2\text{O}=0.53-0.62$), with rare earth spectra enriched in light-rare earth elements ($\text{La/Yb})\text{N}=9.71\ 10.98$). The origin of the dacite is linked to the early geological evolution of the eastern sector of the Trans-Mexican Volcanic Belt (TMVB) during the Miocene, and its provenance could be a melt of a basaltic and pelitic-sediments slab and magmatic differentiation that generated adakitic magma. The gem-type corundum could have resulted after the addition of refractory products disaggregated from the Precambrian basement, carried, and transported to the surface by ascending magma.

Key words: Ruby, corundum, dacite, xenocrystals, Mexico, state of Hidalgo.

Resumen

Se consigna la ocurrencia de xenocristales anhédrales de corindón rojo (rubí) de 1-2 cm de diámetro, en un derrame lávico dacítico del centro de México (estado de Hidalgo). Geoquímicamente, la dacita presenta algunos rasgos de roca adakítica ($\text{SiO}_2=63.73\ 66.64\ \text{wt \%}$), con bajo contenido en alúmina ($\text{Al}_2\text{O}_3=14.38\ 14.93\ \text{wt \%}$), sodio ($\text{Na}_2\text{O}=3.29\ 3.57\ \text{wt \%}$) y titanio ($\text{TiO}_2=0.55\ 0.60\ \text{wt \%}$), ligeramente peraluminosa ($\text{A/CNK}=1.04\ 1.17$) y medianamente potásica ($\text{K}_2\text{O}=1.90\ 2.04\ \text{wt \%}$; $\text{K}_2\text{O}/\text{Na}_2\text{O}=0.53\ 0.62$), con espectros de tierras raras enriquecidos en tierras raras ligeras ($\text{La/Yb})\text{N}=9.71\ 10.98$). El origen de la dacita está ligada a la evolución geológica temprana del sector oriental de la Faja Volcánica Transmexicana, durante el Mioceno, y podría provenir de la fusión de losa basáltica-sedimentos pelíticos y diferenciación magmática para constituir una lava adakítica. El corindón variedad gema sería el resultado de la incorporación de productos refractarios disgregados de basamento precámbrico, acarreados y transportados a la superficie por la lava en ascenso.

Palabras clave: Rubí, corindón, dacita, xenocristales, México, estado de Hidalgo.

Received: June 14, 2023; Accepted: March 26, 2024; Published on-line: July 1, 2024.

Editorial responsibility: Dr. Gustavo Murillo Muñetón

* Corresponding author: José Cruz Escamilla Casas, jocesca@uaeh.edu.mx.

¹ Universidad Autónoma del Estado de Hidalgo, Instituto de Ciencias Básicas e Ingeniería, Área Académica de Ciencias de la Tierra y Materiales Mineral de la Reforma, Hidalgo, México.

² leoh@uaeh.edu.mx

Luis Enrique Ortiz Hernández, José Cruz Escamilla Casas

<https://doi.org/10.22201/igeof.2954436xe.2024.63.3.1727>

1. Introduction

Corundum is a relatively scarce mineral on our planet. Its gem varieties -sapphires and rubies- are much scarcer because they are formed at 10-40 km terrestrial depth (Stern *et al.*, 2013) from where they are transported to the surface as xenocrystals or xenoliths in alumina-rich, silica-poor igneous rocks (Giuliani *et al.*, 2014; Giuliani *et al.*, 2020). Also, the occurrence of corundum is in metamorphic rocks (Wilson, 1974; Baumgartner *et al.*, 2001) and some placer deposits (Simonet *et al.*, 2008).

While iron, titanium, and nickel trace contents in sapphires result in a wide range of colors -yellow, green, blue, orange, black and pink- ruby chromophores derive from trace chromium (Al_3 substituted by Cr_3+ in the crystalline structure) (García-Lastra *et al.*, 2005) and are less common than rubies with traces of vanadium or iron (Dubinski *et al.*, 2020) which result in rubies ranging in color from orange-red to purplish-red. In Mexico, the presence of sapphire xenocrystals has been documented in an Oligocene andesitic dike ($\text{K}/\text{Ar} = 29.20 \pm 0.30$ 30.50 ± 0.60 Ma; Ortega-Gutiérrez *et al.*, 2011). However, up until now, the occurrence of rubies has not been reported in the Mexican territory (e. g. Cruz-Ocampo *et al.*, 2007).

The aim of this work is to document, for the very first time, their occurrence and discuss the possible origin of gem-type red corundum (ruby) in Mexico, particularly in the eastern sector of the Trans-Mexican Volcanic Belt (TMVB) which crosses the middle of the state of Hidalgo (central Mexico) from east to west.

1.1. Analytical Methods

Due to their scarcity, fieldwork was carried out seeking rock samples containing xenocrystals, which were later prepared for petrographic analysis. Although fresh samples lack xenocrystals, they can be found in altered rocks. Thin sections were cut along different orientations to determine the texture and any dacite constituents; subsequently, samples were studied and photographed under a Leitz BA310 polarizing microscope at the Laboratory of Petrography at the Universidad Autónoma del Estado de Hidalgo (UAEH).

Three rock samples (PT-1, PT-2 and PT3) were selected for whole-rock geochemical analysis. These samples were pulverized for analysis preparation -major and trace elements- with a 200-mesh using an agate mortar at the Servicio Geológico Mexicano. The analyses were conducted with 95% confidence on a Phillips MagixPRO X-Ray fluorescence spectrometer and a Palma Quad-3 being, induced coupled plasma mass spectrometer (ICPMS).

1.2. Regional geology and outcrop description

In central Mexico, the southern portion of the state of Hidalgo

is geologically dominated by the TMVB (Figure 1), which is a relatively young geological province (Miocene-Quaternary) with its eastern sector characterized by discrete volcanic fields, and predominance of andesitic lava and dacitic flows, domes, pyroclastic flows, cineritic cones, and calderas. Among them, the most important are Apan-Tezontepec volcanic field (García-Palomo *et al.*, 2002), Apan- Tecocomulco (García-Tovar *et al.*, 2015), Xihuingo-La Paila (Valadez-Cabrera, 2012), Chichicaultla-Tecocomulco (Juárez-López, 2015), Epazoyucan-Singuilucan (Aparicio-Canales & Contreras-Cruz, 2016), San Vicente (Ramírez-Ramírez, 2016) and Las Navajas (Núñez-Velázquez, 2018). These volcanic fields engulf, in variable proportion, Early to Medium-Late Miocene rocks, forming pyroclastic deposits, lava flows, domes and, eventually, calderas. After a magmatic ~7 Ma hiatus during the Pliocene, coupled with bimodal vulcanism occurred the emplacement of lava spills, pyroclastic flows, and cineritic cones (García-Tovar *et al.*, 2015).

For a portion of the Sierra de Pachuca, Martínez-González (2018) recently proposed the existence of three volcanic events: the lower formed by Oligocene to early Miocene dacitic and andesitic lava flows and domes; a middle event formed by early to mid-Miocene rhyolitic ignimbrites and pyroclastic deposits; and an upper event formed by mid-Miocene andesitic lava flows and domes. Very likely, the country rock that hosts ruby xenocrystals belongs to the first volcanic event proposed by Martínez-González (2018) and in this case, it will be placed between 23.70 21.60 Ma, equivalent to the K/Ar radiometric age reported by Geyne *et al.* (1990) for the rocks in the local stratigraphic column corresponding to the Santa Gertrudis-Zumate formations.

The area of the outcrop is about 4 km² and constitutes a 10 m column of pseudostratified dacitic lava spill, slightly tilted to the SE. The rock is tan, gray to cream, occasionally red due to sericitic alteration and oxidation; also affected by NW-SE and NE-SW trending normal faults and abundant joints. Xenocrystals are anhedral, 1-2 cm in diameter, are scarce, and occupy 1 % of the rock (Figure 2). This dacite discordantly overlaps andesitic flows, domes, and breccias of the Pachuca Group (Geyne *et al.*, 1963) and it is overlaid by lapilli tuff.

2. Petrography and Geochemistry

The lava host rock contains the typical dacitic mineralogy with subhedral plagioclase phenocrystals of medium to sodic composition and partial sericitic alteration; hornblende and biotite are accessory minerals embedded in a microlithic matrix of sanidine, interstitial glass, seldom quartz, and disseminated iron-titanium oxides. Amphiboles altered to opaques and/or hematite at the rim, and biotite is altered to chlorite. Ruby xe-



Figure 1. Location map of the state of Hidalgo and geologic provinces (TMVB = Trans-Mexican Volcanic Belt, VSLPP= Valles-San Luis Platform, MFTB=Mexican Folds and Thrust Belt, GMM=Gulf of Mexico Miogeoclinal). In the inset a map of central Mexico shows the subdivision of the TMVB in three sectors (western, central, and eastern), geologic provinces and adjacent tectonostratigraphic terranes (Sedlock *et al.*, 1993); MGP = Morelos-Guerrero Platform. Location of the principal volcanoes are indicated by asterisks: San Martin (Sm), Pico de Orizaba (Po), La Malinche (Ma), Iztaccíhuatl (Iz), Popocatépetl (Pp), Nevado de Colima (Vc), and Ceboruco (Ce). Circles indicate the active calderas: Los Humeros (LH), Los Azufres (LA), and La Primavera (LP). Localities of lower-crust xenoliths represented by small solid diamonds are in Pico de Orizaba, Iztaccíhuatl, Popocatépetl, and La Malinche (Ortega-Gutiérrez *et al.*, 2008). Large solid diamonds indicate the localities where xenoliths have been found in granulite facies rocks: Puente Negro (Pn), Chalcatzingo (Cha), Pepechucha (Pe), Amealco (Am), and Valle de Santiago (Vs) (Ortega-Gutiérrez *et al.*, 2011). A black solid star with the Rx label indicates the locality in the eastern sector of the TMVB where the dacite containing ruby xenocrystals have been found. An open star with a Mo label indicates the locality, to the north, where the Precambrian basement crops out.

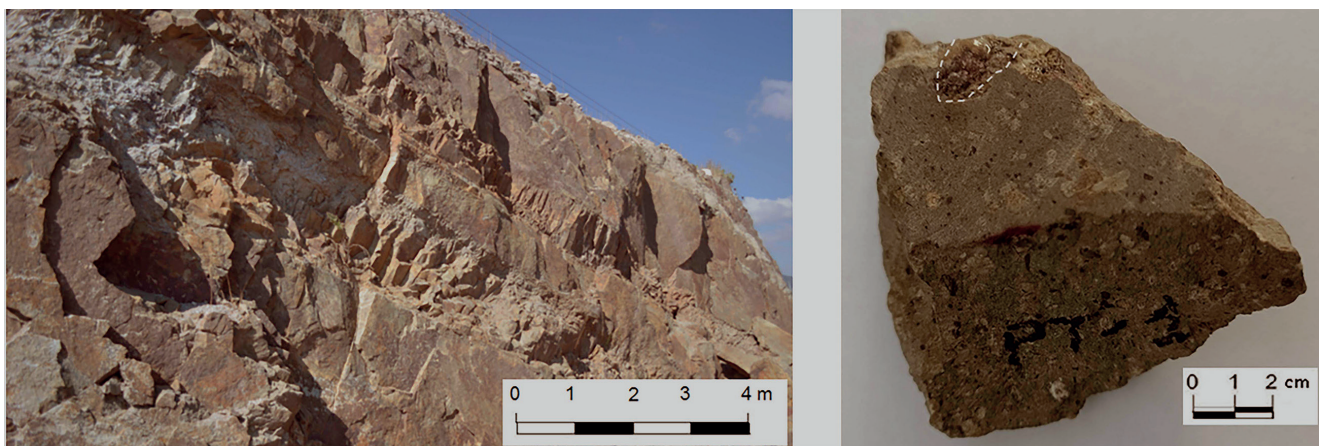


Figure 2. Photographs showing the outcropping dacitic lava host rock and a rock sample of centimeter scale ruby xenocrystals (Dotted half circle). The lava flow is pseudostratified, altered, and jointed.

nocrystals are anhedral, fractured, and scarce; present high relief, low birefringence, with abundant undetermined inclusions and an incipient diaspora alteration (Figure 3) suggesting corundum hydration. The rock is classified as hornblende-biotite dacite.

From the geochemical perspective, the three samples analyzed for major, and some trace elements (Table 1) exhibit typical dacite features, with SiO_2 contents between 63.73–66.64 wt % (Figure 4a) with low alumina contents ($14.38 \text{ wt\%} \leq \text{Al}_2\text{O}_3 \leq 14.93 \text{ wt\%}$), sodium ($3.29 \text{ wt\%} \leq \text{Na}_2\text{O} \leq 3.57 \text{ wt\%}$) and titanium ($0.55\% \leq \text{TiO}_2 \leq 0.60 \text{ wt\%}$). It is a slightly peraluminous rock ($1.04 \leq \text{A/CNK} \leq 1.17$) (Figure 4b), moderately potassic ($1.90 \text{ wt\%} \leq \text{K}_2\text{O} \leq 2.04 \text{ wt\%}$), trondhjemetic ($0.53 \leq \text{K}_2\text{O}/\text{Na}_2\text{O} \leq 0.62$) and differentiated ($43 \leq \# \text{Mg} \leq 47$).

CIPW analysis (not shown) presents as normative minerals, quartz, plagioclase, orthoclase, hypersthene, and corundum (1.00–2.82 wt %).

Some geochemical characteristics of the studied dacite resemble adakitic rock (Zhang *et al.*, 2019), for example $\text{SiO}_2 > 56 \text{ wt\%}$, $\text{MgO} < 3 \text{ wt\%}$, $\text{TiO}_2 < 0.60 \text{ wt\%}$, $\text{Y} < 18 \text{ ppm}$, $\text{Yb} < 1.80 \text{ ppm}$ (Defant & Drummond, 1990; Drummond & Defant, 1990; Drummond *et al.*, 1996; Martin *et al.*, 2005; Sun *et al.*, 2012) and the ratios $\text{Y/Yb} \sim 10$ y $\text{Dy/Yb} (1.79-1.84)$, suggesting residual amphibole and garnet. Rare earth total sum varies between 91.50–100.90 ppm, with $(\text{La/Yb})_{\text{N}} = 9.71-10.98$ ratio (normalization values of Sun & McDonough, 1989).

Light rare earth values (La, Ce, Nd, Sm, and Gd) are closer to the earth crust total values (17.60–20.90 ppm vs 20 ppm, 39.40–41.60 ppm vs 43.73 ppm, 15.40–18.30 ppm vs 19.81 ppm, 3.00–3.30 ppm vs 3.93 ppm and 3.30–3.70 ppm vs 3.83 ppm, respectively (Rudnick & Gao, 2003), as well as the ratio $\text{U/Th} = 0.22-0.24$ vs 0.25 (Rudnick & Fountain, 1995). While the $\text{Sm/Nd} = 0.18-0.19$ ratio is very close to mid continental crust ($\text{Sm/Nd} = 0.18$; Rudnick & Fountain, 1995).

Dacitic flow Gd/Yb ratio is higher than 1 (2.54–2.69) suggesting a source involving garnet. The Yb/Lu coefficient varies between 6.50–7.00 which is higher than silica rich adakites ($\text{HSA} \sim 5$; Moyen, 2009). La/Yb ratio varies between 13.53–15.31 falling in the range of modern continental margin adakites ($\text{La/Yb} < 50$; Sun *et al.*, 2012) but it is lower than silica rich adakites ($\text{La/Yb} \sim 20$; Moyen, 2009). $\text{Sm/Yb} = 2.31-2.46$ and $\text{La/Sm} = 5.80-6.30$ fall in the range of adakites ($\text{Sm/Yb} = 3-7$ and $\text{La/Sm} = \sim 2-10$; Dimalanta & Yumul, 2008).

The Europium anomaly is not so evident ($\text{Eu/Eu}^* = 1.1-1.16$), while the Cerium anomaly ($\text{Ce/Ce}^* = 0.91-1.05$), which is close to 1, is common in rocks associated with subduction. This value of Ce/Ce^* suggests the contribution of pelagic clay sediments (Elliot *et al.*, 1997; Hastie *et al.*, 2010; Bellot *et al.*, 2018). Furthermore, present island arcs with significant volume of subducted sediments typically show $\text{Th/Yb} \geq 2$ ratios (Nebel *et al.*, 2007; Woodhead *et al.*, 2001;). In support of the later, this ratio in the studied samples varies between 3.30–3.40.

On a $(\text{La/Yb})\text{N}$ vs YbN diagram, the studied dacite falls in the non-discriminatory field between “normal” calc-alkaline arc rocks and adakites (Figure 4c). In other binary diagrams (not shown) like Th/Ce vs Th , the studied dacite falls in the field of Cenozoic slab derived adakite; La/Th diagram vs Yb/Gd strongly points to a magmatic arc setting (Ueki *et al.*, 2022), while the $(\text{Na}_2\text{O}+\text{K}_2\text{O})/(\text{FeO}+\text{MgO}+\text{TiO}_2)$ vs $\text{Na}_2\text{O}+\text{K}_2\text{O}+\text{FeO}+\text{MgO}+\text{TiO}_2$ diagram suggests that this dacite comes from partial melt amphibolite.

On a Th vs SiO_2 diagram (Wang *et al.*, 2006), this dacite is associated with the field of adakites derived from subducted oceanic crust (Figure 4d). This fact is also corroborated on the $\text{K}_2\text{O}/\text{Na}_2\text{O}$ vs Al_2O_3 diagram (Figure 4e).

Finally, the rare earth elements diagram normalized with respect to chondrites (normalization values of Sun & McDonough, 1989; Figure 4f) shows light rare earth enrichment

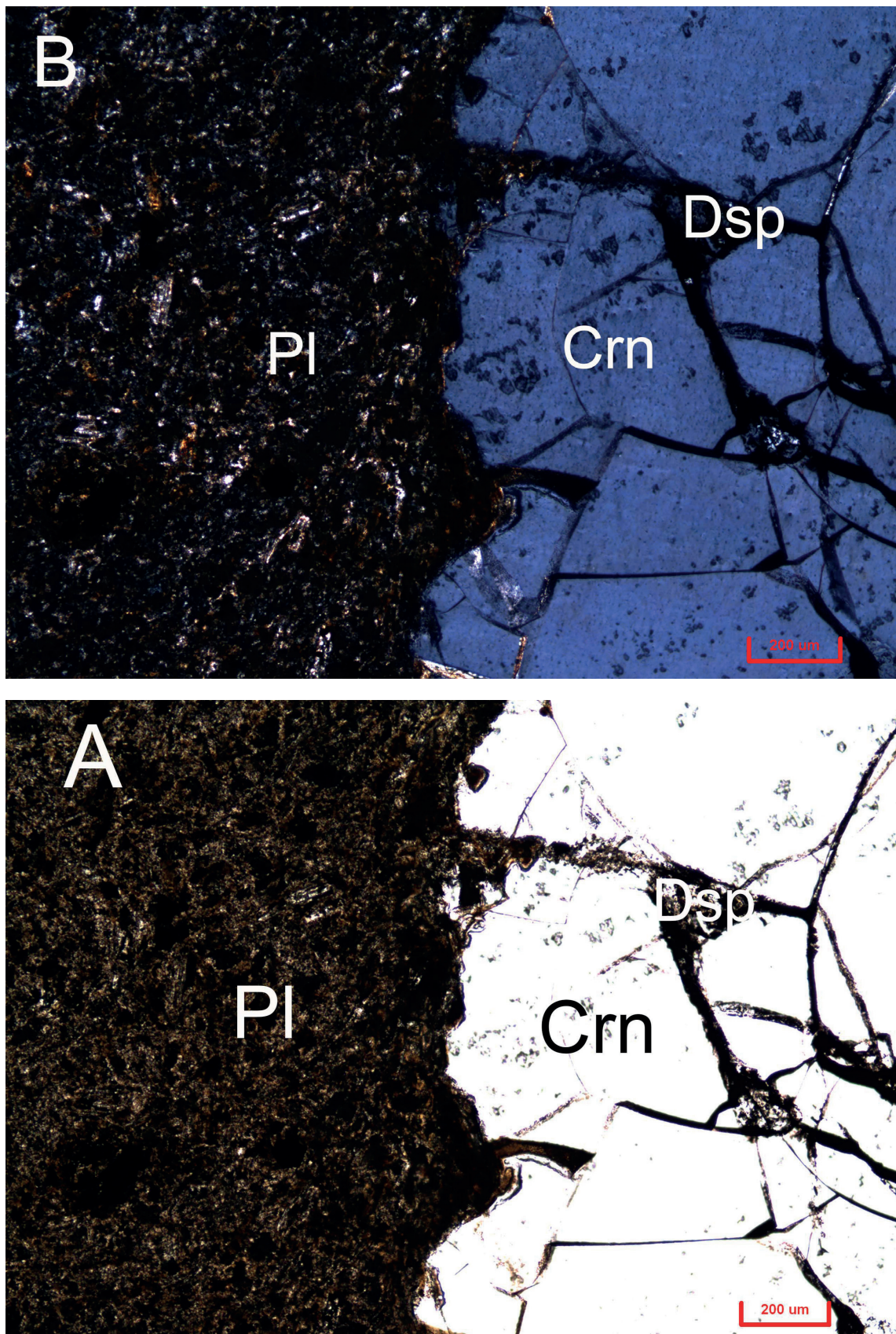


Figure 3. Photomicrographs showing the petrographic characteristics of the studied dacite and ruby xenocrystals, 5X; A = PPL; B = XPL. Plagioclase phenocrystals (Pl), are observed with partially vitreous microlithic matrix and fractured anhedral ruby phenocrystals (Crn) with incipient alteration to diasporite (Dsp).

Table 1. Whole rock chemical analysis (wt %) and some trace elements (ppm) of three dacite rock samples.

Sample	PT-1	PT-2	PT-3	Sample	PT-1	PT-2	PT-3
SiO ₂	63.73	66.00	66.64	Th	4.50	4.40	4.60
Al ₂ O ₃	14.93	14.56	14.38	U	1.10	1.00	1.00
Fe ₂ O ₃	3.4	3.46	3.09	Y	13.00	13.20	13.80
MgO	1.64	1.36	1.26	La	17.60	19.90	20.90
CaO	3.54	2.70	2.66	Ce	40.30	39.40	41.60
Na ₂ O	3.57	3.29	3.33	Pr	4.20	4.70	5.00
K ₂ O	1.90	2.04	2.04	Nd	15.40	17.40	18.30
TiO ₂	0.60	0.58	0.55	Sm	3.00	3.20	3.30
P ₂ O ₅	0.17	0.18	0.17	Eu	1.20	1.20	1.30
MnO	0.07	0.09	0.05	Gd	3.30	3.50	3.70
LOI	5.15	5.21	5.10	Tb	0.50	0.50	0.50
Total	98.70	99.47	99.27	Dy	2.40	2.40	2.50
				Ho	0.50	0.50	0.50
				Er	1.4	1.4	1.5
				Tm	0.20	0.20	0.20
				Yb	1.30	1.30	1.40
				Lu	0.20	0.20	0.20

and a negative slope from La to Lu, indicating heavy rare earth depletion with respect to light rare earth elements, a common geochemical feature of subduction associated rocks (Pearce, 1983; Rollinson, 1993).

3. Formation conditions

Despite lacking quantitative mineralogical data of glass or mineral composition in the dacite, formation conditions of the studied rock were determined based on whole rock chemical composition. As such, a temperature range of 829–877 °C was obtained for the liquidus with Norm4 (Hollocher, 2004), while the thermometer proposed by Jung & Pfander (2007) based in the Al₂O₃/TiO₂ ratio, yielded a temperature range between 925–928 °C. The former range of temperature (829–877 °C) is considered more reliable for dacite formation. Additionally, other parameters were established using Norm4 (Hollocher, 2004), the magma density (2.74–2.75 g/cm³) and magma water contents (3–3.50 wt %).

Based on the geochemistry of some trace elements, mohometric methods were applied to establish the crustal depth of formation of the dacite such as the La/Yb ratio. This is because Dimalanta & Yumul (2008) proposed that the La/Yb ratios in adakitic rocks can be applied as an approach to investigate crustal thicknesses, so that a La/Yb=10 ratio represents 30–35 km

thickness and a La/Yb=10–20 ratio a crustal thickness greater than 42 km. In our study, La/Yb ratio is in the 13.80–15.30 range, consequently a crust thickness greater than 42 km is considered.

Furthermore, using the La/Yb ratio and applying the equation proposed by Sundell *et al.* (2021) after Profeta *et al.* (2015), where H represents the crustal depth ($H = 17.0 \times \ln(\text{La/Yb}) + 6.9$), a value of crustal thickness of 26–27 km is obtained. On the other hand, the calculated depth using Ce/Y ratio and the equation proposed by Mantle & Collins (2008) ($H = 18.0505 \times \ln(\text{Ce/Y}) + 21.5587$) a range of 30–30.4 km is obtained. The above-mentioned depths are concordant with the crustal thickness of 45–50 km determined for the eastern sector of the TMVB (Ferrari *et al.*, 2012; Urrutia-Fucugauchi & Flores-Ruiz, 1996).

4. Discussion

According to Stern *et al.* (2013) ruby deposits are good petrogenetic markers, indicative of continental collision, formed at amphibolitic or granulitic facies or from fusion of Al rich and silica poor protoliths, between 10 to 40 km crustal depth. Due to these facts, many ruby and sapphire deposits are found close to ancient continental margins and subduction zones (Wong & Verdel, 2017). Several geologic settings propitiate the occurrence of rubies, such as: 1) amphibole or granulite facies metamorphic belts (Dahanayake & Ranasinghe, 1981; Kriegsman &

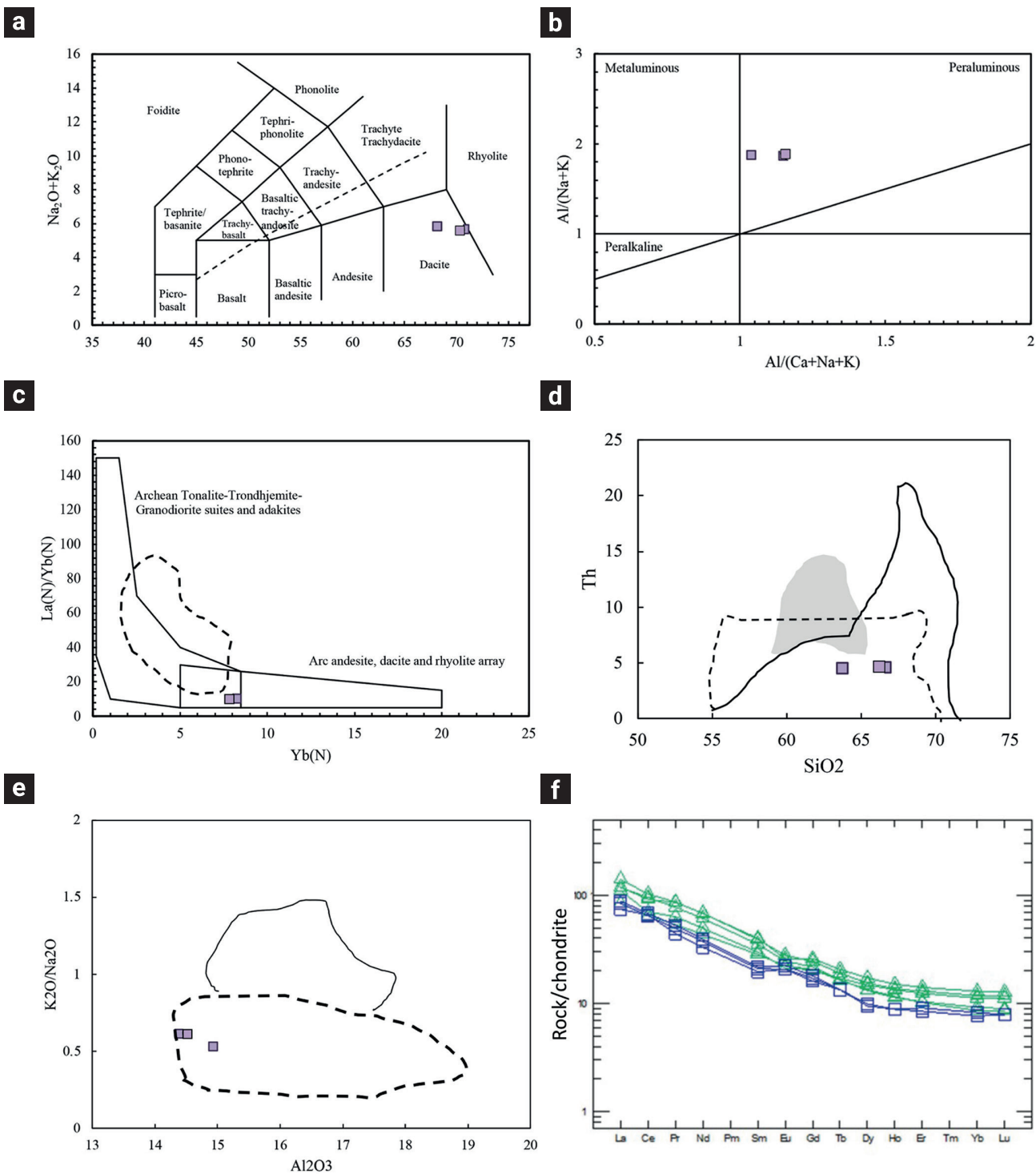


Figure 4. a) SiO₂ vs Na₂O+K₂O diagram showing the host rock classification, b) its peraluminous character according to the CAN/K vs ANK diagram, and c) the non-discriminatory field between arc calc-alkaline rocks and adakites (dotted line shows the field of metabasaltic rock after experimental studies in equilibrium with eclogitic residuals; Rapp *et al.*, 2003), d) Th vs SiO₂ diagram (Wang *et al.*, 2006) showing that the studied rock samples belong to adakite derived from subducted oceanic crust (dotted line), differing from adakite derived from lower delaminated crust (dark field) and from adakite derived from thick oceanic crust (continuous line). e) K₂O/Na₂O vs Al₂O₃ diagram showing the classification of the dacite as adakite derived from subducted oceanic crust (dotted line; Kamei *et al.*, 2009) which is different from adakite derived from thick oceanic crust (continuous line; Liu *et al.*, 2010). f) rare earth elements normalized diagram with respect to chondrites (normalization values of Sun & McDonough, 1989) showing enrichment in light rare earth elements, typical of subduction associated rocks. Also shown, for comparison purposes, the spectrum of rare earth elements of the Sierra de Pachuca lower volcanic event (triangles, Martínez-González, 2018) with similar spectra, but enriched in rare earth elements ((La/Yb)_N=7.47 12.90).

Schumacher, 1999), 2) settings of alkali basalt associated with subduction zones, involving oceanic and continental plates (Levinson & Cook, 1995), 3) continental rift zones related to alkali basalt volcanism (Giuliani *et al.*, 2020), and 4) placer deposits associated with sedimentation (Dill, 2018).

For the studied ruby, the formation setting is interpreted as, firstly, to be associated with the early geologic history of the TMVB during the Miocene -considered as the age of formation for the host rock- and secondly, that constitutes the basement of the eastern sector of the TMVB.

As stated by Ortega-Gutiérrez *et al.* (2008) the lower crust of the TMVB and surrounding setting to the south, must be at granulite facies, with a minimum temperature between 700 800 °C, a crustal thickness about 40 45 km, and with the presence of garnet at the deepest levels. Nonetheless, higher temperatures for the granulite facies (950 112 °C) have been proposed for central Mexico (Hayob *et al.*, 1989) and 990 1100 °C for southern Mexico (Ortega-Gutiérrez *et al.*, 2011).

It is accepted that the occurrence of granulitic outcrops and xenoliths coming from the lower crust have been reported in Mexico (Hayob *et al.*, 1989; Roberts & Ruiz, 1989; Ruiz *et al.*, 1988). In central Mexico (TMVB and surroundings) in five localities, granulite facies xenoliths have been thoroughly studied even though they can be present in several other places (e.g., Pico de Orizaba, Carrazco-Núñez *et al.*, 2005). Two of the localities are in the central portion of the TMVB (e.g., Valle de Santiago, see Gutiérrez *et al.*, 2014; Urrutia-Fucugauchi & Uribe-Cifuentes, 1999; and Amealco, see Aguirre-Díaz *et al.* 2002) which

are basic granulites. The remaining three localities are found in adjacent areas to the south (forearc): Pepechuca (Elías-Herrera & Ortega-Gutiérrez, 1997), Puente Negro (Ortega-Gutiérrez *et al.*, 2011) and Chalcatzingo (Ortega-Gutiérrez *et al.*, 2012), which are pelitic granulites constituted by pyrope rich garnet, sillimanite, rutile, spinel, corundum, cordierite, orthopyroxene, and Fe-Ti oxides with less common quartz and feldspar.

On these occurring granulitic xenoliths localities, it has been proposed the existence of Precambrian basement of which a nearby outcrop is documented in Molango, Hidalgo -Huiznopala gneiss- at ~75 km far from the eastern sector of the TMVB (Figure 1) and characterized by the presence of ortho-and para-gneiss, and a gabbro-anorthositic complex (Lawlor *et al.*, 1999).

According to Ortega-Gutiérrez *et al.* (2008), the eastern sector of the TMVB could be underlain by Grenvillian basement rocks (~1Ga), belonging to the Oaxaquia micro-continent (Ortega-Gutiérrez *et al.*, 1995), and constituted by metapelites, quartzofeldspathic gneisses, calc-silicates, amphibolites, and marbles intruded by anorthosites, charnockites, and garnetiferous mafic gneisses. The whole lithologic sequence is metamorphosed to granulite facies and locally re-equilibrated to amphibolite facies.

As stated by Ortega-Gutiérrez *et al.* (2008), the reported granulites might be representative of the upper part (25 30 km depth) of the lower Precambrian crust, affected by Cenozoic thermal processes including the emplacement of contemporaneous mafic magma (underplating), metamorphic granulite facies, partial melting, and magma mixing. This fact is concordant with

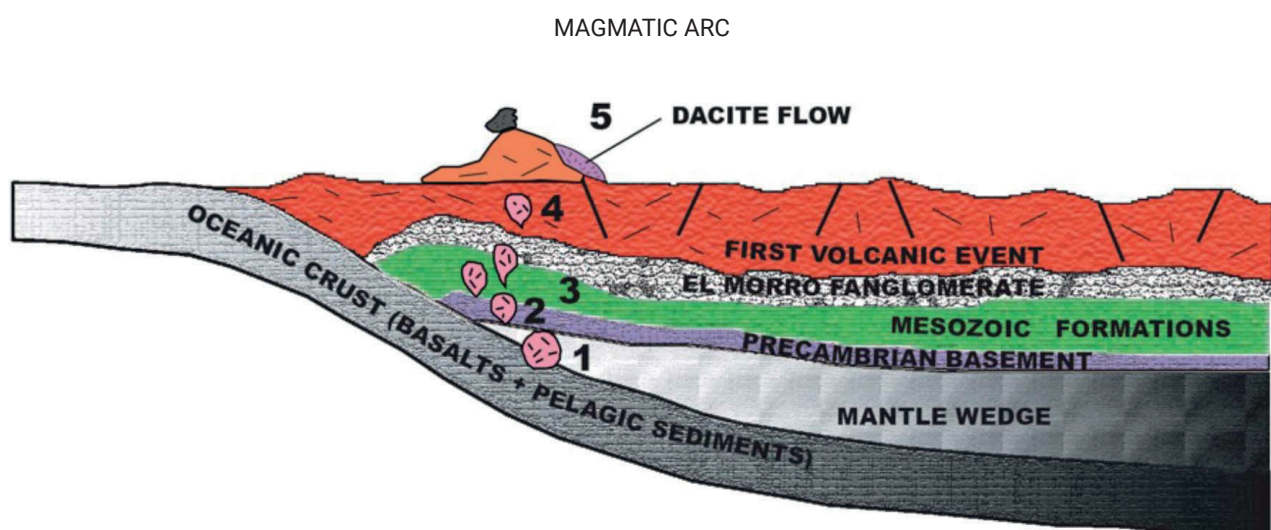


Figure 5. Schematic simplified model explaining the origin of ruby crystals: 1) formation of basaltic magma emplaced at the mantle wedge, 2) diapiric ascension of adakitic magma, 3) magmatic differentiation and assimilation of Precambrian rock xenocrystals, 4) constant ascension reaching shallow levels of the crustal arc, and 5) spill of the dacite lava containing ruby xenocrystals.

the mohometric results based on La/Yb and Ce/Y (26–27 km and 30–30.40 km, respectively).

Under these conditions, the dacite could have originated after partial melting of the basaltic lava and pelagic clay sediments -giving the rock a peraluminous character, the $\text{Ce}/\text{Ce}^* \pm 1$ anomalies, and $\text{Th}/\text{Yb} \geq 2$ ratio- on an arc geologic setting, as it is described by Drummond & Defant (1990) and Drummond *et al.* (1996) for adakites and for silica rich adakites (Martin *et al.*, 2005; Moyen, 2009) very likely favored by a sub horizontal subduction, as it has been suggested for the eastern and central sectors of the TMVB (Gómez-Tuena *et al.*, 2003; Mori *et al.*, 2007).

Xenocrystals of red corundum (rubi), which are refractory products, may come from: a) fusion of pelagic clay sediments subducted during the formation of dacitic magma, b) from pelitic and calcareous Cretaceous formations which constitute the bedrock of the Sierra de Pachuca (e.g., El Doctor, Mexcala and Méndez formations, see Geyne *et al.*, 1963), or c) the presumable Precambrian basement of the TMVB, which could correspond to metapelitic, amphibolitic, or marble rock fragments, that were disintegrated and accidentally incorporated into the ascending dacitic magma (Figure 5). From the above-mentioned, the hypothesis involving a Precambrian basement is considered the most viable.

Fractured ruby crystals and the presence of opaques and hematite at the rim of amphibole phenocrystals in the dacite host rock, may result from sudden adiabatic decompression during quick lava ascension (Devine *et al.*, 1998), while the incipient diasporite alteration of the xenocrystals, suggests corundum hydration and disequilibrium (Voudouris *et al.*, 2009) very likely produced by hydrothermalism.

5. Conclusions

This work confirms the occurrence of red corundum xenocrystals (ruby), in an early Miocene dacitic flow with adakitic affinity in the eastern sector of the TMVB. Despite its occurrence in a small outcrop (4 km^2) and the scarce presence of xenocrystals, it is highly likely that exist more outcrops of adakitic rocks with xenocrystals or xenoliths from the lower crust, which will shed light into the understanding of the bedrock and geodynamic evolution of the Sierra de Pachuca. For interpretation purposes, the source of xenocrystals found is interpreted as the Precambrian basement of the eastern sector of the TMVB.

On the other hand, this first report of the presence of ruby in rocks of the Sierra de Pachuca, strongly suggests that the rocks in this locality not only host world class metallic ore deposits but, likely, deposits of different kind.

6. References

- Aguirre-Díaz, G. J., Dubois M., Laureyns J., & Schaaf, P. (2002) Nature and P-T conditions of the crust beneath the Central Mexican Volcanic Belt based on a Precambrian crustal xenolith. *International Geology Review*, 44(3), 222–242. doi: <https://doi.org/10.2747/0020-6814.44.3.222>
- Aparicio-Canales, O., & Contreras-Cruz, D. (2016). *Caracterización petrográfica y geoquímica de las rocas volcánicas del área de Epazoyucan-Singilucan, estado de Hidalgo* [Tesis de Licenciatura], Universidad Autónoma del Estado de Hidalgo.
- Bellot, N., Boyet, M., Doucelance, R., Bonnand, P., Savov, I. P., Plank, T., & Elliott, T. (2018). Origin of negative cerium anomalies in subduction-related volcanic samples: Constraints from Ce and Nd isotopes. *Chemical Geology*, 500, 46–63. doi: <https://doi.org/10.1016/j.chemgeo.2018.09.006>
- Baumgartner, L. P., Fernando, G. W. A. R., Hauzenberger, C. A., & Hofmeister, W. (2001 April 4–10). A Metamorphic Petrologist's View on Gemstone Formation: An Example from Sri Lanka. *Proceedings of the International Workshop on Material Characterization by Solid State Spectroscopy: The Minerals of Vietnam*, Hanoi.
- Carrasco-Nuñez, G., Righter, K., Chesley, J., Siebert L., & Aranda-Gómez, J. J. (2005). Contemporaneous eruption of calc-alkaline and alkaline lavas in the continental arc (Eastern Mexican Volcanic Belt): chemically heterogeneous but isotopically homogeneous source. *Mineralogy and Petrology*, 150, 423–440.
- Cruz-Ocampo, J. C., Canet, C., & Peña-García, F. (2007). Las gemas de México. *Boletín de la Sociedad Geológica Mexicana*, LIX(1), 9–18.
- Dahanayake, K., & Ranasinghe, A. P. (1981). Source rocks of gem minerals. A case study from Sri Lanka. *Mineral Deposita*, 16, 103–111.
- Defant M. J., & Drummond, M. S. (1990). Derivation of some modern arc magmas by melting of young, subducted lithosphere. *Nature*, 347, 662–665.
- Devine, J. D., Murphy, M. D., Rutherford, M. J., Barclay, J., Sparks, R. S. J., Young S. R., & Gardner, J. E. (1998). Petrologic evidence for pre-eruptive pressure-temperature conditions, and recent reheating, of andesitic magma erupting at the Soufrière Hills Volcano, Montserrat, W.I. *Geophysical Research Letters*, 25(19), 3669–3672.
- Dill, H. G. (2018). Gems and placers-A genetic relationship par excellence. *Minerals* 8, 470–513.
- Dimalanta, C. B., & Yumul, G. P. Jr. (2008). Crustal thickness and adakite occurrence in the Philippines: Is there a relationship? *Island arc*, 17 (4), 421–431.
- Drummond, M. S., & Defant, M. J. (1990). A model for trondhjemite-tonalite-dacite genesis and crustal growth via slab melting: Archean to modern comparisons. *Journal of Geophysical Research* 95(B13), 21503–21521.
- Drummond, M. S., Defant, & Kepezhinskas, M. J., (1996). Petrogenesis of slab-derived trondhjemite-tonalite-dacite/adakite magmas. *Transactions of the Royal Society of Edinburgh, Earth Sciences*, 87, 205–215.

- Dubinski, E. V., Stone-Sundberg, J., Emmett, J. L. (2020). A quantitative description of the causes of color in corundum. *Gems & Gemology*, 56(1), 2–28. doi: <http://dx.doi.org/10.5741/GEMS.56.1.2>
- Elías-Herrera, M., & Ortega-Gutiérrez, F. (1997). Petrology of high-grade metapelitic xenoliths in an Oligocene rhyolite plug-Precambrian crust beneath the southern Guerrero terrane, México? *Revista Mexicana de Ciencias Geológicas*, 14, 101–109.
- Elliott, T., Plank, T., Zindler, A., White, W., & Bourdon, B. (1997). Element transport from slab to volcanic front at the Mariana arc. *Journal of Geophysical Research*, 102(B7), 14991–15019. doi: <https://doi.org/10.1029/97JB00788>
- Ferrari, L., Orozco-Esquivel, T., Manea, V., & Manea, M. (2012). The dynamic history of the Trans-Mexican Volcanic Belt and the Mexico subduction zone. *Tectonophysics*, 522–523, 122–149. doi: <https://doi.org/10.1016/j.tecto.2011.09.018>
- García-Lastra, J. M., Barriuso, M. T., Aramburu, J. A., & Moreno, M. (2005). Origin of the different color of ruby and emerald. *Physical Review B* 72(113104). doi: <https://doi.org/10.1103/PhysRevB.72.113104>
- García-Palomo, A., Macías, J. L., Tolson, G., Valdez, G., & Mora, J. C. (2002). Volcanic stratigraphy and geological evolution of the Apan region, east-central sector of the Trans-Mexican Volcanic Belt. *Geofísica Internacional*, 41(2), 133–150. doi: <https://doi.org/10.22201/igeof.00167169p.2002.41.2.282>
- García-Tovar, G. P., Martínez-Serrano, R. G., Solé, J., Correa-Tello, J. C., Núñez-Castillo, E. Y., Guillou, H., & Monroy-Rodríguez, E. (2015). Geología, geocronología y geoquímica del vulcanismo Plio-Cuaternario del campo volcánico Apan-Tecocomulco, Faja Volcánica Trans-Mexicana. *Revista Mexicana de Ciencias Geológicas*, 32, 100–122.
- Geyne, A. R., Fries Jr., C., Segerstrom K., Black R. F., & Wilson I. F. (1963). *Geology and mineral deposits of the Pachuca-Real del Monte district, State of Hidalgo, Mexico*. Consejo de Recursos Naturales No Renovables, publication 5E.
- Geyne, A. R., Fries Jr., C., Segerstrom, K., Black, R. F., & Wilson, I. F. (1990). Geology and mineral deposits of the Pachuca-Real del Monte district, Hidalgo, México. In *Silver deposits of Mexico, Geological Society of America Bulletin*, 241–258.
- Giuliani, G., Groat, L. A., Fallick, A. E., Pignatelli, I., & Pardieu, V. (2020). Ruby Deposits: A Review and Geological Classification. *Minerals*, 10(7), 597. doi: <https://doi.org/10.3390/min10070597>
- Giuliani G., Ohnenstetter D., Fallick A. E., Groat L. A., & Fagan A. J. (2014). The geology and genesis of gem corundum deposits. In L. A. Groat (Ed.), *Geology of Gem Deposits* (2nd ed., 29–112). Mineralogical Association of Canada, Short Course Series 44.
- Gómez-Tuena, A., LaGatta, A., Langmuir, C., Goldstein, S., Ortega-Gutiérrez, F., & Carrasco-Núñez, G. (2003). Temporal control of subduction magmatism in the Eastern Trans-Mexican Volcanic Belt: mantle sources, slab contributions and crustal contamination. *Geochemistry, Geophysics, Geosystems*, 4(8), 8912. doi: <https://doi.org/10.1029/2003GC000524>
- Hastie, A. R., Ramsook, R., Mitchell, S. F., Kerr, A. C., Millar, I. L., & Mark, D. F. (2010). Geochemistry of Compositionally Distinct Late Cretaceous Back-Arc Basin Lavas: Implications for the Tectonomagmatic Evolution of the Caribbean Plate. *The Journal of Geology*, 118(6), 655–676. doi: <https://doi.org/10.1086/656353>
- Hayob, J. L., Essene, E. J., Ruiz, J., Ortega-Gutiérrez, F., & Aranda-Gómez, J. J. (1989). Young high-temperature granulites from the base of the crust in central Mexico. *Nature*, 342, 265–268.
- Hollocher, K. (2004). *CIPW Norm Calculation Program*. Geology Department, Union College.
- Juárez-López, K. (2015). *Evidencias de procesos magnéticos: Caracterización geoquímica e isotópica (Sr, Nd y Pb) del Campo Volcánico Chichicuacatl-Tecocomulco, Estado de Hidalgo* [Tesis de Maestría] Universidad Nacional Autónoma de México.
- Jung, S., & Pfänder, J. A. (2007). Source composition and melting temperatures of orogenic granitoids—constraints from CaO/Na₂O, Al₂O₃/TiO₂ and accessory mineral saturation thermometry. *European Journal of Mineralogy* 19(6), 859–870. doi: <https://doi.org/10.1127/0935-1221/2007/0019-1774>
- Kamei, A., Miyake, Y., Owada, M., & Kimura, J. I. (2009). A pseudo adakite derived from partial melting of tonalitic to granodioritic crust, Kyushu, southwest Japan arc. *Lithos*, 12, 615–625.
- Kriegsman, L. M., & Schumacher, J. C. (1999). Petrology of sapphirine-bearing and associated granulites from central Sri Lanka. *Journal of Petrology*, 40, 1211–1239.
- Lawlor, P. J., Ortega-Gutiérrez, F., Cameron, K. L., Ochoa-Camarillo, H., Lopez, R., & Sampson, D. E. (1999). U-Pb geochronology, geochemistry, and provenance of the Grenvillian Huiznopala Gneiss of eastern Mexico. *Precambrian Research*, 94, 73–99.
- Levinson, A. A., & Cook, F. A. (1995). Gem corundum in alkali basalt: origin and occurrence. *Gems & Gemology*, 30(4), 253–262.
- Liu, S. A., Li, S. G., He, Y. S., & Huang, F. (2010). Geochemical contrasts between early Cretaceous ore-bearing and ore-barren high-Mg adakites in central-eastern China: Implications for petrogenesis and Cu-Au mineralization. *Geochimica et Cosmochimica acta*, 74, 7160–7178.
- Mantle, G. W., & Collins, W. J. (2008). Quantifying crustal thickness variations in evolving orogens: Correlation between arc basalt composition and Moho depth. *Geology*, 36(1), 87–90. doi: <https://doi.org/10.1130/g24095a.1>
- Martin, H., Smithies, R. H., Rapp, R., Moyen, J. F., & Champion, D. (2005). An overview of adakite, tonalite-trondhjemite-granodiorite (TTG), and sanukitoid: relationships and some implications for crustal evolution. *Lithos* 79, 1–24.
- Martínez-González, I. R. (2018). Aportaciones petrográficas, geoquímicas e isotópicas en la caracterización petrogenética de rocas volcánicas de la sierra de Pachuca. [Tesis de Licenciatura]. Universidad Nacional Autónoma de México.
- Mori, L., Gómez-Tuena, A., Cai, Y., & Goldstein, S. (2007). Effects of prolonged flat subduction on the Miocene magmatic record of the central Trans-Mexican Volcanic Belt. *Chemical Geology*, 244, 452–473.
- Moyen, J. F. (2009). High Sr/Y and La/Yb ratios: the meaning of the

- "adakitic signature". *Lithos*, 112, 556–574.
- Nebel, O., Münker, C., Nebel-Jacobsen, Y. J., Kleine, T., Mezger, K., & Mortimer, N. (2007). Hf–Nd–Pb isotope evidence from Permian arc rocks for the long-term presence of the Indian–Pacific mantle boundary in the SW Pacific. *Earth and Planetary Science Letters* 254, 377–392.
- Núñez-Velázquez, M. V. (2018). Volcán Las Navajas estado de Hidalgo: características geoquímicas e isotópicas del magmatismo peralcalino en la Faja Volcánica Transmexicana. [Tesis de Licenciatura]. Universidad Nacional Autónoma de México.
- Ortega-Gutiérrez, F., Elías-Herrera, M., & Dávalos-Elizondo, M. G. (2008). On the nature and role of the lower crust in the volcanic front of the Trans-Mexican Volcanic Belt and its fore-arc region, southern and central Mexico. *Revista Mexicana de Ciencias Geológicas*, 25, 346–364.
- Ortega-Gutiérrez, F., Elías-Herrera, M., Gómez-Tuena, A., Mori L., Reyes-Salas, M., Macías-Romo, C., & Solari, L. A. (2012). Petrology of high-grade crustal xenoliths in the Chalcatzingo Miocene subvolcanic field, southern Mexico: buried basement of the Guerrero-Morelos platform and tectonostratigraphic implications. *International Geology Review* 54(14), 1597–1634.
- Ortega-Gutiérrez, F., Gómez-Tuena, A., Elías-Herrera, M., Reyes-Salas, M., & Macías-Romo, C. (2014). Petrology and geochemistry of the Valle de Santiago lower-crust xenoliths: Young tectonothermal processes beneath the central Trans-Mexican volcanic belt. *Lithosphere*, 6(5), 335–360. doi: <https://doi.org/10.1130/L317.1>
- Ortega-Gutiérrez, F., Martíny B. M., Morán-Zenteno, D. J., Reyes-Salas, A. M., & Solé-Viñas, J. (2011). Petrology of very high temperature crustal xenoliths in the Puente Negro intrusion: a sapphire-spinel-bearing Oligocene andesite, Mixteco terrane, southern Mexico. *Revista Mexicana de Ciencias Geológicas*, 28(3), 593–629.
- Ortega-Gutiérrez, F., Ruiz, J., & Centeno-García, E. (1995). Oaxaquia, a Proterozoic microcontinent accreted to North America during the late Paleozoic. *Geology*, 23(12), 1127–1130.
- Pearce, J. A. (1983). Role of the sub-continental lithosphere in magma genesis at active continental margins. In C. J. Hawkesworth & M. J. Norry (Eds.), *Continental basalts and mantle xenoliths*. Shiva Publications, 230–249.
- Profeta, L., Ducea, M. N., Chapman, J. B., Paterson, S. R., Gonzales, S. M. H., Kirsch, M., Petrescu, L., & DeCelles, P.G. (2015). Quantifying crustal thickness over time in magmatic arcs. *Scientific Reports*, 5, 17786. doi: <https://doi.org/10.1038/srep17786>
- Ramírez-Ramírez, B. B. (2016). Campo volcánico San Vicente, estado de Hidalgo, Faja Volcánica Trans-mexicana: variaciones geoquímicas e isotópicas y su relación con el retroceso del arco hacia la trinchera. [Tesis de Licenciatura]. Instituto Politécnico Nacional, ESIA-Unidad Ticomán.
- Rapp, R. P., Shimizu, N., & Norman, M. D. (2003). Growth of early continental crust by partial melting of amphibolite. *Nature*, 425, 605–809.
- Roberts, S. J., Ruiz, J. (1989). Geochemistry of Exposed Granulite Facies Terrains and Lower Crustal Xenoliths in Mexico. *Journal of Geophysical Research*, 94(B6), 7961–7974.
- Rollinson, H. (1993). *Using geochemical data: evaluation, presentation, interpretation*. Pearson.
- Rudnik, R. L., & Fountain, D. M. (1995). Nature and composition of the continental crust: a lower crustal perspective. *Reviews of Geophysics* 33(3), 267–309.
- Rudnick, R. L., & Gao, S. (2003). Composition of the continental crust. In *Treatise on Geochemistry*, 3, 1–64. Elsevier Ltd.
- Ruiz, J., Patchett, P. J., & Ortega-Gutiérrez, F. (1988). Proterozoic and Phanerozoic basement terranes of Mexico from Nd isotopic studies. *Geological Society of America Bulletin*, 100, 274–281.
- Sedlock, R. L., Ortega-Gutiérrez, F., & Speed, R. C. (1993). Tectonostratigraphic terranes and tectonic evolution of Mexico. *Geological Society of America Special Paper*, 278, 1–153.
- Simonet, C., Fritsch, E., & Lasnier, B. (2008). A classification of gem corundum deposits aimed towards gem exploration. *Ore Geology Reviews*, 34, 127–133.
- Stern, R. J., Tsujimori, T., Harlow, G., & Groat, L. A. (2013). Plate tectonic gems, *Geology*, 41(7), 723–726. doi: <https://doi.org/10.1130/G34204.1>
- Sun, S., & McDonough, W. F. (1989). Chemical and isotopic systematics of oceanic basalts: implications for mantle composition and processes. *Geological Society, London, Special Publications*, 42(1), 313–345.
- Sun, W. D., Ling, M. X., Chung, S. L., Ding, X., Yang, X. Y., Liang, H. Y., Fan, W. M., Goldfarb, R., & Yin, Q. Z. (2012). Geochemical constraints on adakites of different origins and copper mineralization. *The Journal of Geology*, 120, 105–120.
- Sundell, K. E., Laskowski, A. K., Kapp, P. A., Ducea, M. N., & Chapman, J. B. (2021). Jurassic to Neogene quantitative crustal thickness estimates in southern Tibet. *Geological Society of America Today*, 31(6), 4–10. doi: <https://doi.org/10.1130/gsatg461a.1>
- Ueki K, Hino H., & Kuwatani T. (2022). Extracting the geochemical characteristics of magmas in different global tectono-magmatic settings using sparse modeling. *Frontiers in Earth Sciences*, 10. doi: <https://doi.org/10.3389/feart.2022.994580>
- Urrutia-Fucugauchi, J., Flores-Ruiz, J. (1996). Bouguer gravity anomalies and regional crustal structure in central Mexico. *International Geology Reviews*, 38, 176–194.
- Urrutia-Fucugauchi, J., Uribe-Cifuentes, R. M. (1999). Lower-crustal xenoliths from the Valle de Santiago maar field, Michoacán-Guanajuato volcanic field, central Mexico. *International Geology Review*, 41, 1067–1081.
- Valadez-Cabrera, S. (2012). Caracterización petrológica del Campo volcánico Xihuingo-La Paila, Estado de Hidalgo: Evidencias Geoquímicas e Isotópicas de Sr, Nd y Pb [Tesis de Maestría]. Universidad Nacional Autónoma de México.
- Voudouris, P., Mavrogenatos, C. Graham, C. J., Giuliani, G., Melfos, V., Karampelas, S., Karantoni, V., Wang, K., Tarantola, A., Zaw, K., Meffre, S., Klemme, S., Berndt, J., Heidrich, S., Zaccarini, F., Fallick, A., Tsortanidis, M., & Lampridis, A. (2009). Gem corundum deposits of Greece: Geology, mineralogy and genesis. *Minerals*, 9(1), 49. doi:

<https://doi.org/10.3390/min9010049>

Wang, Q., Xu, J. F., Jian, P., Bao, Z. W., Zhao, Z. H., Li, C. F., Xiong, X. L., & Ma, J. J. (2006). Petrogenesis of adakitic porphyries in an extensional tectonic setting, Dexing, south China: implications for the genesis of porphyry copper mineralization. *Journal of Petrology*, 47, 119–144.

Wilson, A.F. (1974). The mineral potential of granulite terranes and other highly metamorphosed segments of the earth's crust. *Annales de la Société géologique de Belgique*. Publications spéciales special publications, Géologie des domaines cristallins - Centenaire de la Société géologique de Belgique, 301–321. Recuperado de: <https://popups.ulege.be/0037-9395/index.php?id=3732>

<https://popups.ulege.be/0037-9395/index.php?id=3732>

Woodhead, J. D., Hergt, J. M., Davidson, J. P. & Eggins, S. M. (2001).

Hafnium isotope evidence for ‘conservative’ element mobility during subduction processes. *Earth and Planetary Science Letters* 192, 331–346.

Wong, J., & Verdel, C., 2017. Tectonic environments of sapphire and ruby revealed by a global oxygen isotope compilation. *International Geology Review*, 60(2), 188–195. doi: <https://doi.org/10.1080/00206814.2017.1327373>

Zhang, L., Li S., Zhao, Q., 2019. A review of research on adakites. *International Geology Review*, 1-18. doi: <https://doi.org/10.1080/0206814.2019.1702592>